

RESEARCH ARTICLE



Stem cell-derived extracellular vesicles mitigate ageing-associated arterial stiffness and hypertension

Rui Feng^a, Mujib Ullah^b, Kai Chen^b, Quaisar Ali^b, Yi Lin^b and Zhongjie Sun^b

^aDepartment of Cardiology, The First Affiliated Hospital of Chongqing Medical University, Chongqing, China; ^bDepartment of Physiology, College of Medicine, University of Tennessee Health Sciences Center, Memphis, TN, USA

ABSTRACT

The prevalence of arterial stiffness and hypertension increases with age. This study investigates the effect of induced pluripotent mesenchymal stem cell-derived extracellular vesicles (EVs) on ageing-associated arterial stiffness and hypertension. EVs were collected and purified from induced pluripotent stem cell-derived mesenchymal stem cells (iPS-MSCs). Young and old male C57BL/6 mice were used. Mice in the EVs group were injected *via* tail vein once a week for four weeks (18×10^6 EVs/mouse/injection). Blood pressure (BP) was measured using the tail-cuff method and validated by direct cannulation. Pulse wave velocity (PWV) was measured using a Doppler workstation. PWV and BP were increased significantly in the old mice, indicating arterial stiffness and hypertension. Intravenous administration of EVs significantly attenuated ageing-related arterial stiffness and hypertension, while enhancing endothelium-dependent vascular relaxation and arterial compliance in the old EVs mice. Elastin degradation and collagen I deposition (fibrosis) were increased in aortas of the old mice, but EVs substantially improved ageing-associated structural remodelling. Mechanistically, EVs abolished downregulation of sirtuin type 1 (SIRT1), and endothelial nitric oxide synthase (eNOS) protein expression in aortas of the older mice. In cultured human aortic endothelial cells, EVs promoted the expression of SIRT1, AMP-activated protein kinase alpha (AMPK α), and eNOS. In conclusion, iPS-MSC-derived EVs attenuated ageing-associated vascular endothelial dysfunction, arterial stiffness, and hypertension, likely *via* activation of the SIRT1-AMPK α -eNOS pathway and inhibition of MMPs and elastase. Thus, EVs mitigate arterial ageing. This finding also sheds light into the therapeutic potential of EVs for ageing-related vascular diseases.

Abbreviations: EV: Extracellular vesicles; iPS: induced pluripotent stem cell; MSC: mesenchymal stem cell; AMPK α : AMP activated protein kinase α ; eNOS: endothelial nitric oxide synthase; Sirt1: sirtuin 1; JNC7: Seventh Report of the Joint National Committee; CVD: cardiovascular disease; PWV: pulse wave velocity; BP: blood pressure; SNP: sodium nitroprusside

ARTICLE HISTORY

Received 17 August 2019
Revised 1 February 2020
Accepted 24 April 2020

KEYWORDS



Extracellular vesicles; stem cell; arterial stiffness; hypertension; SIRT1; AMPK


Introduction

The human life span has significantly increased over recent decades and is expected to increase even further, but so too is the prevalence of age-related cardiovascular disease and the development of arterial stiffness and hypertension [1,2]. The Framingham Heart Study has shown that even people who are normotensive (what is typically considered “normal” BP) at age 55 still have a 90% risk of eventually developing hypertension during their lifetime. In addition, according to the Seventh Report of the Joint National Committee (JNC7), more than two-thirds of individuals aged 65 years or older suffer from hypertension [3]. Hypertension is also an

independent risk factor for many cardiovascular diseases including coronary artery disease, ventricular dysfunction, and heart failure [4].

Ageing-related hypertension is associated with alterations in a number of structural and functional properties of large arteries, including diameter, wall thickness, wall compliance, and endothelial function. The wall of large arterial vessels, especially the aorta, become stiffer with age because of gradual fragmentation and degradation of elastin and subsequent deposition of collagen fibres [5,6]. Arterial stiffness precedes the development of hypertension, and more frequently in the elderly [7,8]. Numerous studies have demonstrated that arterial stiffness is an independent

CONTACT Zhongjie Sun  Zsun10@uthsc.edu  Department of Physiology, College of Medicine, University of Tennessee Health Sciences Center Memphis, TN 38163, USA

 Supplemental material for this article can be accessed [here](#).

© 2020 The Author(s). Published by Informa UK Limited, trading as Taylor & Francis Group on behalf of The International Society for Extracellular Vesicles. This is an Open Access article distributed under the terms of the Creative Commons Attribution-NonCommercial License (<http://creativecommons.org/licenses/by-nc/4.0/>), which permits unrestricted non-commercial use, distribution, and reproduction in any medium, provided the original work is properly cited.

predictor of hypertension and related cardiovascular disorders such as ischaemic heart disease, stroke, and chronic kidney diseases [8–11]. It has been reported that arterial stiffness is independently associated with decline in kidney function (chronic kidney disease) [9–11]. Arterial stiffness has also been shown to indicate a higher risk of incident hypertension [12–14]. Therefore, it is important to control arterial stiffness. Yet current antihypertensive drugs are mainly designed to reduce peripheral resistance and are not adequate to alter the pathological process of vascular stiffening.

Accumulating evidence has shown that extracellular vesicles (EVs), which originate from diverse subcellular compartments and are released in the extracellular space [15], have emerged as crucial regulators of vascular homeostasis and cardiovascular disease (CVD) progression such as myocardial infarction and heart failure. By transferring biological messages to target vascular cells, EVs have emerged as novel regulators of intercellular communication between adjacent and remote cells [16]. Because vesicle composition and biological content are specific signatures of cellular activation and injury, their potential as diagnostic and prognostic biomarkers have raised significant interest with researchers working in the field of cardiovascular disease [15,17,18].

Induced pluripotent stem cells (iPS cells) are somatic master cells that have been successfully used to “reprogram” human cells to a state very similar to embryonic stem cells (ESCs) [19]. iPS cells offer tremendous therapeutic potential because they come from a patient’s own cells, thus eliminating problems with tissue matching and tissue rejection. Furthermore, iPS cells are considered as a valuable alternative to the more controversial usage of ESCs that involves human embryos [20,21]. Studies have suggested that EVs derived from stem cells may deliver specific signals to the microenvironment, regulating cell proliferation and differentiation, as well as promoting tissue regeneration [22,23]. A particular iPS derivative, mesenchymal stem cells (iPS-MSCs), has been shown to be an especially attractive option for use in cell replacement therapy and treatment of a variety of diseases including ischaemia and cardiomyopathy.

In this study, we investigated whether the treatment with iPS-MSC-derived EVs could reduce age-related arterial stiffness and hypertension. We also addressed deficiencies in knowledge by focusing on identifying the effects and underlying molecular mechanisms of EVs effect on ageing-related arterial stiffness [24], hypertension, and renal damages.

Methods

Animals

This study was performed according to National Institutes of Health (NIH) guidelines on the care and use of laboratory animals and was approved by the Institutional Animal Care and Use Committee (IACUC) of the University of Oklahoma Health Science Centre. Briefly, 20 wild type mice with C57B/6 background were used. All mice were housed in cages at room temperature (25 ± 1 °C) and were provided with chow diet and tap water.

For the interventional study, 10 young mice (6 months old) and 10 old mice (20 months old) were divided into two groups depending on age. Blood pressure (BP) was measured weekly by a tail cuff non-invasive BP monitoring system. In order to minimize handling stress, mice were gently handled and trained until no signs of stress were observed during BP monitoring. After their BP was stabilized, each group was further divided into two subgroups of five mice (five young EVs, five old EVs, five young control, five old control). Tail vein injection was performed once a week for four weeks. We chose a moderate dose of EVs based on the published dose range used in the *in vivo* studies [25–28]. One subgroup received EVs (18×10^6 /mouse/injection), while the control subgroup received an equal volume of phosphate buffered solution (PBS) and served as a control. Following delivery of EVs, BP was measured twice a week and pulse wave velocity (PWV) measured every other week. Two weeks after the last injections, direct BP for each subgroup (EVs and control) was measured via cannulation under anaesthesia and the animals were then sacrificed (Figure 1(a)). Tissues were collected and prepared for Western blot and immunohistochemical analysis.

Cell culture for human induced pluripotent stem cell-derived mesenchymal stem cells (iPS-MSCs)

Human iPS-MSCs were cultured in α -minimum essential medium (α -MEM; Gibco), 10% (vol/vol) FBS (Atlanta Biologicals), 100 units/mL penicillin (Gibco), 100 μ g/mL streptomycin (Gibco), and 2 mM L-glutamine (Gibco). After 70% confluence in 7 days, cells were washed with PBS (Gibco) and collected by incubation with 3 mL of 0.25% trypsin and 1 Mm EDTA (Gibco) for 3–4 min at 37°C. The harvested cells were replated at 1000 cells per square centimetre in culture dishes (~ 150 cm²) and expanded until

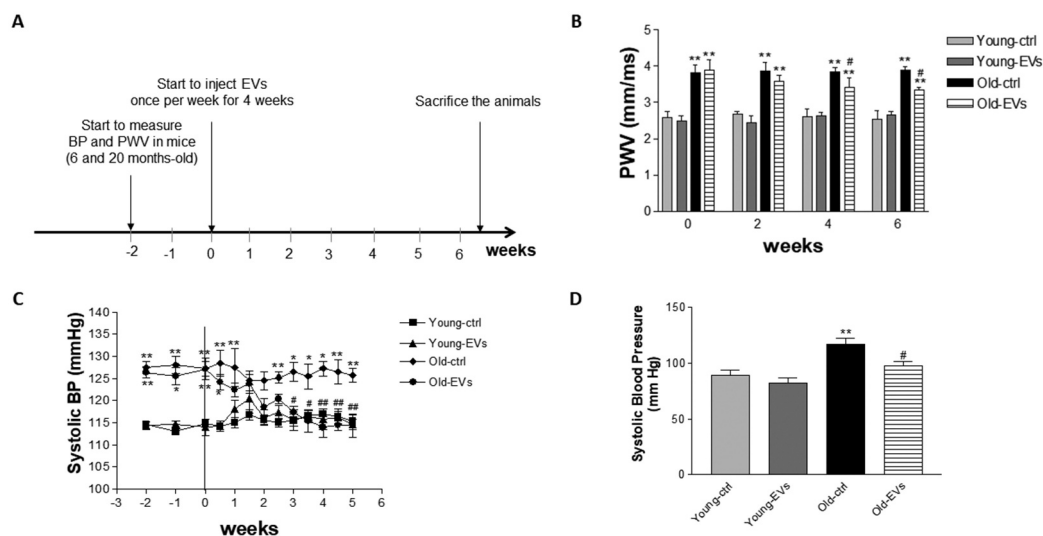


Figure 1. EVs treatments attenuated arterial stiffness and hypertension in old mice.

Schema of experimental designs (A). PWV of arterial flow (B). Arterial systolic BP measured via tail cuff (C) and cannulation (D). Data = means \pm SEM. n = 5. *p < 0.05, **p < 0.01 vs young-ctrl (ND); #p < 0.05, ##p < 0.01 vs old-ctrl.

passage 3. Culture medium was changed every 2 d and 24 h before harvesting the cells for experiments. For all studies, iPS-MSCs were expanded in CCM in a humidified atmosphere at 37°C in 5% O₂. Then the cells were washed at least three times with PBS (Gibco), and the medium was replaced with bovine serum-deficient (1%) and EVs-depleted medium. The depletion was achieved by ultracentrifugation at 100 K \times g in a 45Ti rotor (Beckman, USA), for 8 h.

Transfection of induced pluripotent stem cells (iPS-MSCs)

A lentiviral vector construct, pLenti-SRCMV_i-GFP for expressing green fluorescence protein-GFP, was used for tracking EVs. GFP is a tagging protein. Human induced pluripotent stem cells (iPS-MSCs, passage 3) were cultured and transfected with a multiplicity of infection (MOI) of 10 to 20 as we described previously [29]. In the transfected cells, overexpression of GFP was achieved by using fourth generation lentiviral-based transfer of GFP gene (iPS-MSCs-GFP). GFP was used as a marker for easy detection and tagging of the transduced target cells and their secreted EVs which have GFP tag.

EVs preparation

Ultracentrifugation of EVs

For EVs isolation, the cells were washed with PBS. To make sure that collected EVs only comes from

iPS-MSCs, EVs were depleted from all solutions and EV collection-media used in the study by ultracentrifugation at 100 K \times g in a 45Ti rotor. Serum-deficient/free medium consisting of Chinese hamster ovary medium HT Supplement, MEM Vitamin Solution, MEM Non-Essential Amino Acids solution, PBS (pH 7.4) (All from ThermoFisher Scientific, USA), was added for 48 h before collection of the conditioned medium. After harvesting the conditioned medium in 50 mL falcon tubes, the medium was centrifuged at 300 \times g for 10 min at 4°C in order to pellet the cells. Supernatant was centrifuged at 2,600 \times g for 20 min at 4°C to remove cellular debris and dead cells. Subsequently, the supernatant was transferred to new tubes and centrifuged in a 45Ti rotor (Beckman, USA) for 6 h at 100 K \times g.

Further purification of EVs by chromatography

Ultra-centrifuged EVs were washed in 45 mL of PBS and recentrifuged at 100 K \times g in a 45Ti rotor for 8 h before being re-suspended in 50 mL of sterile PBS. The re-suspended EVs were passed through a column containing the anion exchange resin (Whatman) (10-mL bed volume) that had been equilibrated with 50 mM NaCl in 50 mM Tris buffer (pH 8.0). The medium was applied at a flow rate of 2.0 mL/min at room temperature. The column resin was washed with 10 volumes of the equilibration buffer and then eluted with 25 volumes of 500 mM NaCl in 50 mM Tris buffer (pH 8.0). EVs were collected in fractions and stored at 4°C.

Final purification, quantification and characterization

For EV purification with immuno-selection, Anti-CD63 (Santa Cruz Biotechnology, Inc), CD9 (Cell Signalling), CD81 (Millipore), and IgG (Millipore) antibodies were coupled with Pierce Protein A Magnetic Beads (Life Technologies) in a ratio of 1 µg of antibody per 100 µL of beads overnight at 4°C. Beads were then washed three times with 500 µL of PBS-0.001% Tween. The eluted protein content of the EVs was assayed by the Bradford method (Bio-Rad) and the concentration and size distribution were measured with a NanoSight LM14 instrument (Malvern Instruments, Malvern, UK). Data were analysed with Nanoparticle Tracking Analysis (NTA) software (v.3.2). About 1×10^6 iPSC cells produced 1.2×10^7 to 1.8×10^7 EVs. Supplemental Figure S1A showed the representative size distribution profiles of EV preparations used in the *in vivo* study. Following this procedure, 15×10^9 EVs were re-suspended in 500 mM NaCl in 50 mM phosphate buffer (pH 7.5). Finally, the EVs fractions (10–15 mL) were pooled, dialysed against PBS (molecular weight cut-off 300 kDa). The purified EVs were positive for CD9, CD63, and CD81 as confirmed by western blot (Supplemental Figure S1B,C). The samples were stored at 4°C in PBS before use.

Measurements of BP

Non-Invasive BP was monitored by a computerized volume-pressure recording (VPR) tail-cuff method (CODA, Kent Scientific BP Monitoring System) described previously [30–32]. At the end of the experiment, BP was assessed from the arcus aorta via direct cannulation of a carotid artery under anaesthesia (1% isoflurane) before euthanasia [33] to further validate BP change.

Measurements of PWV

PWV was measured as described recently [34–36]. PWV of arterial blood flow was measured using a Doppler Signal Processing Workstation (DSPW, Indus Instruments, Houston, TX, USA). Each mouse was taped supine to electrocardiogram (ECG) electrodes on a heated procedure board set to a constant temperature of 37°C (Indus Instruments). A 2 mm diameter, 10-MHz Doppler probe was used. Flows of the aortic arch and abdominal artery were recorded. The distance between the aortic arch and the abdominal artery was measured [30,31]. PWV was calculated using DSPW software.

Ex vivo assessment of mesentery artery reactivity

Vessel bioactivity was assayed in an organ chamber as described previously [29,37]. Briefly, after pre-contraction with norepinephrine (NE, 10^{-6} mol/L), the third-order branches of the mesentery artery rings were infused with acetylcholine (ACh, 1×10^{-9} to 1×10^{-5} mol/L) or sodium nitroprusside (SNP, 1×10^{-9} to 1×10^{-5} mol/L) progressively to induce endothelium-dependent or endothelium-independent relaxation, respectively. Vessel wall tension was recorded by an isometric force transducer. Relaxation responses were defined as the percent relaxation of the pre-contracted diameter, and four vessels were examined in each group.

In vitro measurements of aortic stiffness

Mice were sacrificed by exsanguination *via* cardiac puncture while under isoflurane euthanasia. Aortas were excised and incubated in a myograph chamber (DMT, Inc., Atlanta, GA, USA) containing Ca^{2+} -free physiological saline solution (PSS) for 1 h at 37°C [38]. Intraluminal pressure was applied (0–200 mmHg, in 25 mmHg increments) and external aortic diameter was measured. The observed passive response to increasing pressure in isolated arteries reflected aortic stiffness.

Western blot analyses

Western blot analysis was performed as described previously [39–42]. Briefly, the mouse aorta was cut into pieces and homogenized in 200 µl lysis buffer, containing 1× RIPA buffer, protease inhibitor and phosphatase inhibitor. Sample was put on ice, shaking on the rotator for 1 h, then centrifuged ($14,000 \times g$) for 15 min at 4°C. The supernatant was collected, and the protein concentration was measured. An equal amount of protein (30 µg) was loaded in a gradient SDS-PAGE gel (4–20% ExpressPlus PAGE Gel, GenScript USA Inc. NJ, USA). The gel was running with the voltage of 90–120 V for 70–90 min in MOPS buffer. The protein was transferred onto membrane after separation (the time of transfer time was set as 7 min). The membrane was blocked with 5% BSA blocking buffer in TBST for 1 hour, and then the membrane was incubated overnight (4°C) with primary antibodies against eNOS (BD, 610297), p-eNOS (Cell Signalling, 9571 s), AMPKα (Cell Signalling, 2603 s), p-AMPKα (Cell Signalling, 2535 s), SIRT1 (abcam, ab110304), CD9 (Cell Signalling, D801A), CD63 (ThermoFisher Scientific, Ts63), CD81 (ThermoFisher Scientific, AB2532984) and β-actin (abcam, ab8226). Anti-mouse (Cell Signalling, 7076 s) or anti-rabbit (Cell Signalling,

7074 s) were used as the secondary antibody and was incubated for one hour at room temperature. Relative protein expression was normalized to the expression of β -actin. Specific proteins were detected by chemiluminescent methods using Clarity western ECL substrate (Bio-Rad, Hercules, CA). Protein abundance on western blots was quantified by densitometry using Image lab software (Bio-Rad, Hercules, CA).

For preparing the cell lysis of HAECs, cells were washed with PBS for 2 times and harvested in 200 μ l lysis buffer. Samples were put on ice, shaking on the rotator for 1 h, then centrifuged (14,000 \times g) for 15 min at 4°C. The supernatant was collected, and the protein concentration was measured. An equal amount of protein (30 μ g) was loaded.

Morphologic and immunohistochemical investigations

Paraffin-embedded sections (5 μ m) were processed for immunohistochemical staining [43]. A series of 5 sections of each mouse were examined and photographed using an Olympus BH-L microscope coupled with a digital colour camera. The sections were photographed at equal exposure conditions and magnification (10x, 20x, 40x objective). Semi-quantitative analysis was done using Image-J software (NIH, USA) and NIS-Elements BR 3.0 software.

Immunohistochemical staining

The immunohistochemical procedure was described in our previous studies [44,45]. Following perfusion, kidneys and aortas were fixed overnight with 10% formalin (4 °C) and then embedded with paraffin. Tissue sections were incubated with primary antibodies against Collagen 1 (abcam, ab21286), SIRT1 (abcam, ab110304), and eNOS (BD, 610297). Subsequently, the sections were incubated with a secondary antibody including anti-mouse (Cell Signalling, 7076 s) or anti-rabbit (Cell Signalling, 7074 s) for one hour. The sections stained without primary antibody served as the negative control.

Masson's trichrome staining

Trichrome staining (Sigma-Aldrich, St. Louis, MO) was performed in aorta sections for detecting arterial fibrosis [46]. Blue staining indicated collagen deposition. The percentage of blue-stained collagen area over the total aortic area indicated the relative collagen area fraction.

Elastin staining Verhoeff-Van Gieson (VVG) elastin staining was carried out according to the manufacturer's instruction (Sigma, HT25A). Blue-black staining indicated the elastic fibres. The number of elastic fibre

breaks in the aorta indicated severity of fragmentation and degradation of elastin. Briefly, the number of elastin fibre discontinuation points were counted as elastin fibre breaks. A series of 6 sections were examined for each mouse. Elastin fibre breaks were quantified from 4–5 regions per section. The same threshold was used for each photo to make sure they are comparable. The method for analysing elastin fragmentation points were used and confirmed to be reliable in our previous study [34,36].

Periodic acid schiff (PAS) staining

PAS staining in kidneys was performed using a PAS Staining Reagents System (Sigma-Aldrich, St. Louis, MO) according to the manufacturer's instruction. Mesangial matrix area was defined by the PAS-positive and nuclei-free areas in the mesangium. The glomerular area was defined by tracing along the borders of the capillary loop. Relative mesangial area was defined as the fraction of mesangial matrix area over glomerular area. A collapsed glomerulus was defined as an atrophic and heavy-staining glomerulus without normal structure under the microscope. The average percentage of collapsed glomeruli in all glomeruli was calculated.

Cell culture for human aortic endothelial cells

Human aortic endothelial cells (HAECs) were grown in an endothelial cell basal medium (Lonza, Walkersville, MD) containing 2% foetal bovine serum (FBS), penicillin (100 U/ml), streptomycin (100 μ g/ml), and growth factor. All cells were incubated at 37°C in a humidified atmosphere of 5% CO₂. Cells were used at passage 10, and in all experiments the cells were grown to 70–80% confluence before being treated with different agents.

Cell treatment

After being starved for 4 h without FBS, HAECs were treated with EVs (3.15 \times 10³ EVs/0.1 ml/well, 2 \times 10⁶ cells/well) or an equal volume of PBS (control) for 24 h, respectively. Harvested HAECs were then collected and prepared for Western blot analysis.

Statistical analyses

Data were analysed using a one-way ANOVA. The Newman-Keuls procedure was used to assess differences between means. Data were expressed as mean \pm SEM (n = 5). A probability value with p < 0.05 was considered statistically significant.

Results

EVs attenuated arterial stiffening and hypertension in old mice

PWV, a reliable index of arterial stiffness [47–49], increased significantly in the old control group mice (Figure 1(b)). However, PWV was remarkably reduced in the old EVs mice in the fourth week after EVs injection as compared to old control group mice. This reduction was not observed in either young group. Systolic BP increased significantly in old control group compared to young control group (Figure 1(b)). Following delivery of EVs, the BP of old EVs mice started to decrease in the second week after injection (Figure 1(c)). Notably, the high systolic BP of old EVs mice decreased to the control levels by the third week, which was further confirmed by carotid artery cannulation (Figure 1(d)). Thus, our results revealed that EVs could help decrease arterial stiffening and hypertension in old mice.

EVs improved artery compliance and arterial endothelial function in old mice

Arterial compliance was assessed in isolated aortas using myograph. Pressure-induced increases in aortic diameters and the corresponding percentage of diameter increases were both reduced significantly in old mice (Figure 2(a,b)), indicating material stiffness. After treatment with EVs, this reduction was nearly

abolished (Figure 2(a,b)), suggesting that EVs repair ageing-associated arterial stiffening.

Vascular function was assessed in isolated mesenteric arteries using myograph. Vascular relaxing responses to acetylcholine (Ach) were decreased significantly in old mice (Fig. C), indicating that ageing impairs endothelial function. The reduction in endothelium-dependent relaxation to Ach in old mice was nearly reversed by treatment with EVs (Fig. C), suggesting improvement in ageing-associated endothelial dysfunction. By contrast, endothelium-independent relaxing responses to sodium nitroprusside (SNP, nitric oxide donor) was not altered by ageing or treatment with EVs (Figure 2(d)), indicating that the response of vascular smooth muscle cells to nitric oxide is intact. Taken together, these results revealed for the first time that EVs effectively improved ageing-associated vascular endothelial dysfunction and arterial stiffening.

Biodistribution of EVs and serum renin and angiotensin II levels

EVs contain GFP which can be reliably detected by GFP antibody. IHC staining with GFP antibody is preferable to the detection of fluorescence which avoids non-specific auto fluorescence. GFP staining shows that EVs were distributed in vascular endothelial layer and intima (Supplemental Figure S2). The vascular function test showed improvement in vascular function by treatment with EVs (Figure 2). Therefore, EVs

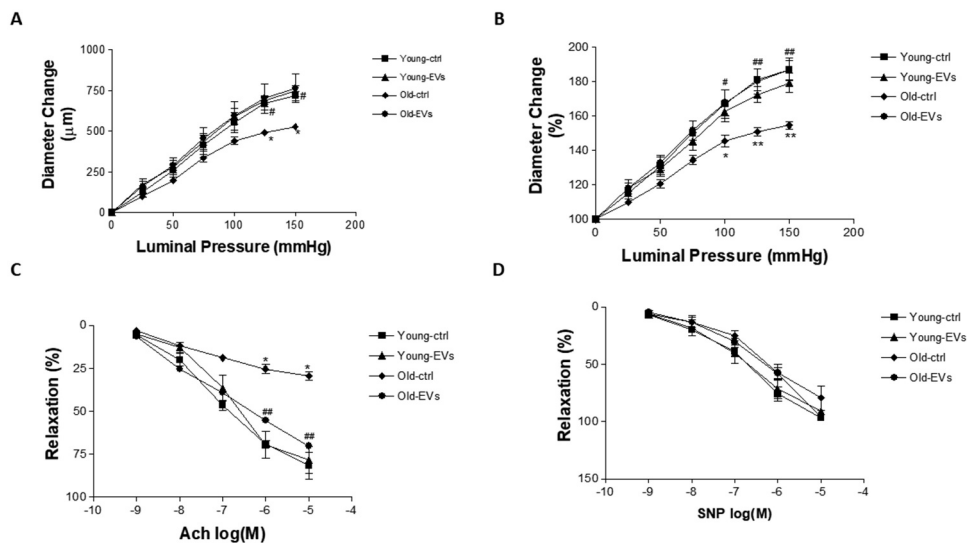


Figure 2. EVs treatments improved arterial compliance and endothelial dysfunction in old mice.

Arterial compliance was assessed by measuring changes in diameter change (A) and percentage of diameter change (B) of aorta following the incremental increase in luminal pressure. Endothelial function was assayed by Ach-induced (C) and SNP-induced (D) relaxation in mesenteric artery. Data = means \pm SEM. n = 5. *p < 0.05, **p < 0.01 vs young-ctrl (ND); #p < 0.05, ##p < 0.01 vs old-ctrl.

improved vascular dysfunction and stiffness at least partially through direct targeting on vascular cells.

Serum renin and angiotensin II (AngII) levels were not affected by either EVs or ageing (Supplemental Figure S3). Therefore, the beneficial effects of EVs on ageing-associated vascular dysfunction, stiffness and remodelling and hypertension may not be mediated by the renin-angiotensin system.

EVs attenuated arterial elastin degradation and collagen deposition in old mice

Elastin degradation and collagen deposition are closely associated with morphological remodelling [50,51]. Elastin staining showed that the number of elastic fibre breaks in the aortic medial layer was markedly increased in old control group mice compared to young control group mice (Figure 3(a,b)). Elastic fibre breaks were significantly attenuated by injection of EVs, suggesting that EVs attenuate arterial elastin degradation in old mice. Significantly increased collagen deposition was observed *via* Masson's trichrome staining in the adventitial layer in aortas in old control mice (Figure 3(c,d)). EV treatment largely attenuated ageing-associated aortic collagen accumulation. Sirius Red staining confirmed building up of collagen in aortas in old mice which

was effectively decreased by EV delivery (Supplemental Figure S4). Specifically, collagen I deposition, which was increased markedly in the adventitial and medial layers as confirmed by immunohistochemistry staining, was abated after injection of EVs (Figure 3(e,f,g)). Based on this data, we concluded that arterial collagen deposition in old mice was attenuated by EVs injection.

EVs rescued the downregulation of SIRT1 protein expression in the aortas of old mice

SIRT1 is a histone deacetylase that regulates expression of genes related to vascular endothelial cell function and is the best characterized mammalian sirtuin. It is highly expressed in the vasculature and is an important modulator of aortic stiffness [34,52]. Interestingly, as immunohistochemistry staining showed, SIRT1 expression in the arterial intima and media layer was decreased significantly in old control group mice and was restored by EVs treatment (Figure 4(a,b,c)). Moreover, in old control group mice, Western blot analysis further confirmed a marked downregulation of SIRT1 expression which was improved in the old EV group mice after treatment (Figure 4(d, e)). Our results thus revealed that EVs rescued the downregulation of SIRT1 protein expression in aortas of old mice.

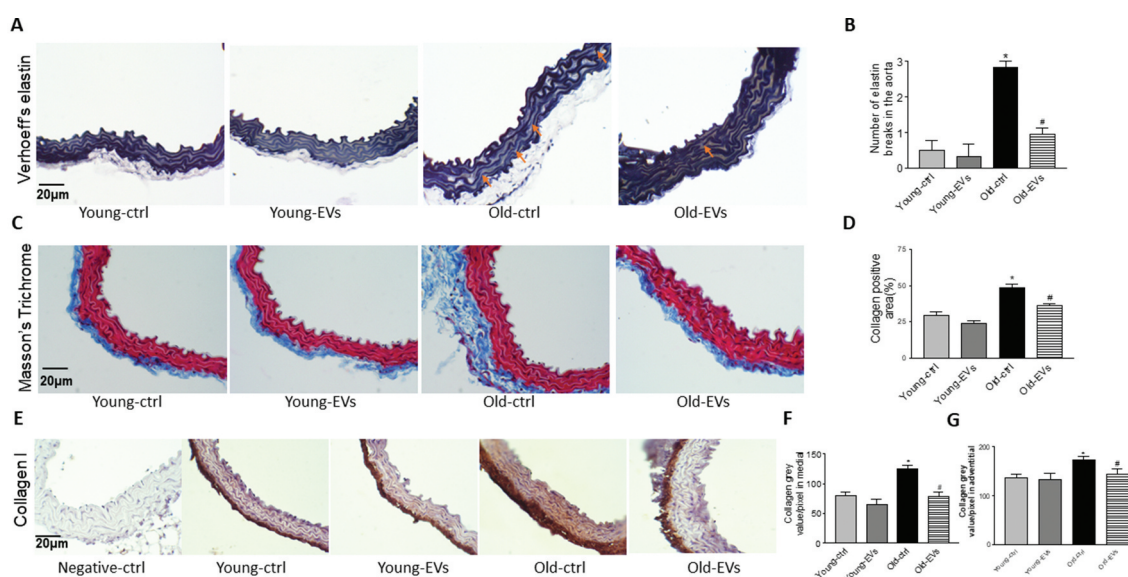


Figure 3. EVs attenuated arterial elastin degradation and collagen deposition in old mice.

Representative images of VVG elastin staining (A) and the number of elastic fibre breaks (B) in aortic sections (arrows indicate breaks in aortic elastic fibres in medium). Representative images of Masson's trichrome staining (C) and the area fraction (D) of collagen deposition in adventitia (blue staining indicating collagen deposition). Representative images of IHC staining of collagen I (E) in aortic sections (brown staining indicates positive staining). Quantitative analysis of collagen I positive staining in aortic media (F) and in adventitia (G). Data = means \pm SEM. n = 5. *p < 0.05, **p < 0.01 vs young-ctrl (ND); #p < 0.05, ##p < 0.01 vs old-ctrl.

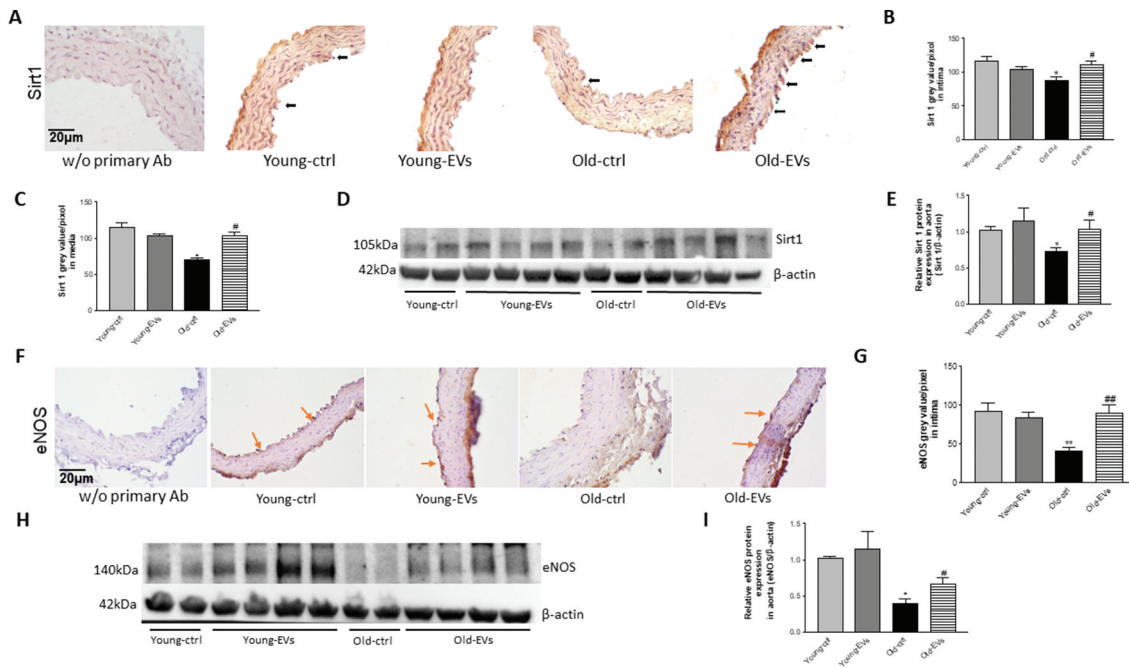


Figure 4. EVs rescued the downregulation of SIRT1 and eNOS protein expression in aortas of old mice.

Representative images of IHC staining of SIRT1 (A) in aortic sections (brown staining indicates positive SIRT1 staining). Semi-quantitative analysis of SIRT1-positive staining in the intima (B) and media (C) of the aortic wall. Representative Western blot bands of SIRT1 (D) and quantitative analysis of SIRT1 protein expression (E) in aortas. Protein expression was normalized to β -actin and the relative expression was calculated as the fold change relative to the young-ctrl group. (F) Representative images of IHC staining of eNOS in aortic sections (brown staining indicates positive staining), and arrows indicate positively stained endothelial cells. Semi-quantitative analysis of eNOS-positive staining in aortic intima (G). Representative Western blot bands (H) and quantitative analysis (I) of eNOS in aortas. Data = means \pm SEM. $n = 5$. * $p < 0.05$, ** $p < 0.01$ vs young-ctrl (ND); # $p < 0.05$, ## $p < 0.01$ vs old-ctrl.

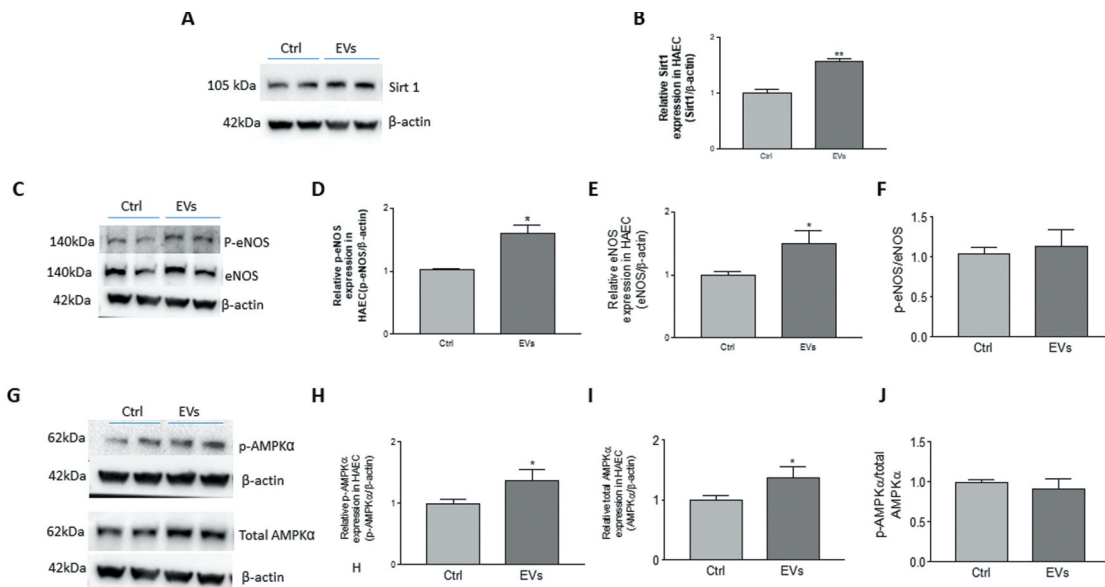


Figure 5. EVs upregulated SIRT1 expression and enhanced eNOS and AMPK α activities in human aortic endothelial cells (HAECs).

Representative Western blot bands (A) and quantitative analysis (B) of SIRT1 in HAECs. Representative Western blot bands (C) and quantitative analysis of p-eNOS and eNOS (D, E, F) in HAECs. Representative Western blot bands (G) and quantitative analysis of p-AMPK α and AMPK α (H, I, J) in HAECs. Protein expression was normalized to β -actin, and the relative expression was calculated as the fold change relative to the control. Data = means \pm SEM. $n = 5$. * $p < 0.05$, ** $p < 0.01$ vs young-ctrl (ND); # $p < 0.05$, ## $p < 0.01$ vs old-ctrl.

EVs enhanced eNOS expression in the aortas of old mice

IHC analysis showed that endothelial nitric oxide synthase (eNOS) proteins were abundantly expressed in endothelial cells (ECs) throughout the intima in old mice treated with EVs (Figure 4(f)). Semi-quantitative analysis further confirmed that eNOS expression was downregulated in the ECs of old mice, which was eliminated by EVs (Figure 4(g)).

We next assessed the protein expression of eNOS by Western blot analysis. Protein expression of eNOS in old control group mice was significantly decreased (Figure 4(h,i)), suggesting that ageing downregulates eNOS expression in the aorta. Interestingly, treatment with EVs abolished the downregulation of eNOS expression in old mice. Taken together, these results suggest that EVs enhance eNOS expression in the aortas of old mice.

EVs upregulated SIRT1 expression in HAECs and enhanced eNOS and AMPK α activity in HAECs

To determine the direct effects of EVs in ECs, we assessed protein expression of SIRT1 (Figure 5(a)), eNOS (Figure 5(c)) and AMP-activated protein kinase (AMPK α) (Figure 5(g)), a serine/threonine protein

kinase that regulates endothelial cell function. The expression of SIRT1 in HAECs increased after EVs treatment (Figure 5(a,b)), indicating that EVs upregulated SIRT1 expression in HAECs. Meanwhile, activity (phosphorylation) of AMPK α and eNOS were also detected. Interestingly, protein expression of phosphorylated AMPK α (p-AMPK α), phosphorylated eNOS (p-eNOS), AMPK α , and eNOS increased in the HAECs treated with EVs (Figure 5(d,e,h,i)). In addition, the ratios of P-AMPK α /AMPK α and P-eNOS/eNOS were not altered in HAECs treated with EVs compared to the control group (Figure 5(f,j)). These results suggest that EVs enhance the expression of active AMPK α and eNOS in HAECs.

EVs attenuated upregulation of TGF- β 1 expression and MMP and elastase activities in aortas in old mice

TGF- β 1 expression was increased in aortas in old mice (Fig. S5). EV treatment significantly attenuated ageing-associated upregulation of TGF- β 1. MMP2 and MMP9 levels were increased in old mice (Fig. S6). Interestingly, EVs attenuated ageing-associated upregulation of MMP levels to the control levels. Elastase activity was increased in aortas in old mice (Fig. S7).

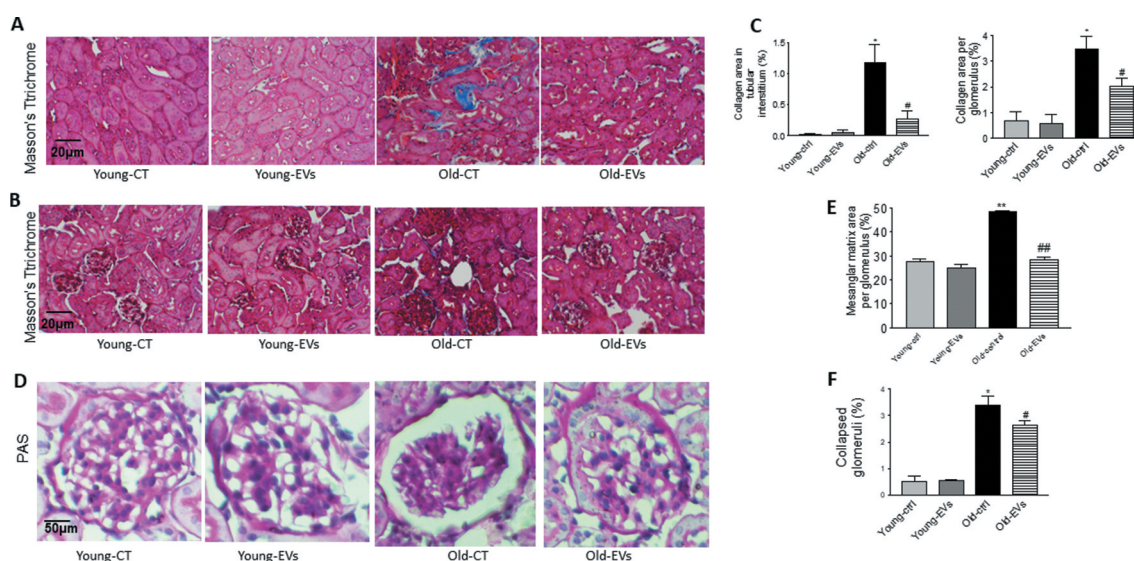


Figure 6. EVs inhibited renal collagen deposition and structural damage in old mice.

Representative images of Masson's trichrome staining of kidney sections. Tubulointerstitial (A) and glomerular fibrosis (B) (blue staining indicating collagen deposition). Semi-quantitative analysis of collagen staining in tubulointerstitium and collagen staining in glomeruli (C). Representative images of Periodic acid-Schiff (PAS) staining glomerulus (D). Semi-quantitative analysis of the average percentage of mesangial matrix area per glomerulus (E). Semi-quantitative analysis of the average percentage of collapsed glomerular number per section in cortex (F). Scale bars, 50 μ m. Data = means \pm SEM. n = 5. *p < 0.05, **p < 0.01 vs young-ctrl (ND); #p < 0.05, ##p < 0.01 vs old-ctrl.

EV treatment largely attenuated ageing-associated upregulation of aortic elastase activity.

EVs inhibited collagen deposition and structural damage in kidneys in old mice

Masson's trichrome staining showed more collagen deposition in the renal tubular interstitia and glomeruli (Figure 6(a,b,c)) of old control group mice versus young control group mice. Renal collagen deposition was significantly attenuated by EVs injection, suggesting that EVs decrease collagen deposition of the glomeruli and attenuate tubulointerstitial nephritis in ageing kidneys. Sirius Red staining confirmed accumulation of collagen in tubular interstitia and glomeruli in old mice which was largely attenuated by EV delivery (Supplemental Figure S8). Meanwhile, significant mesangial matrix expansion and increased collapsed glomerulus in the kidney were also observed *via* PAS staining in the old control group mice (Figure 6(d,e,f)), but were markedly attenuated in the old EVs group mice, indicating that EVs inhibited renal structural remodelling. Renal levels of MMP2 and MMP9 were increased in old mice (Fig. S9). Treatment with EVs attenuated ageing-associated upregulation of MMP2 and MMP9 levels.

Discussion

The prevalence of arterial stiffness and hypertension continues to increase [1,2], especially among the aged population [7]. Our study provides the first evidence that iPS-MSC-derived EVs attenuated ageing-associated arterial stiffness and hypertension *in vivo*. This finding is significant because it offers new insights into the therapeutic strategies for ageing-related arterial stiffness and hypertension.

Endothelia dysfunction, arterial stiffening and hypertension are associated with ageing[7]. It is known that ageing impairs stem cell function [53]. Stem cells could be considered the cellular "fountain of youth." Recent studies showed that stem cells secrete exosomes that play important roles in regulating and maintaining adjacent and remote cells' function [29,54,55]. One of the important findings of this study is that administration of EVs effectively improved endothelial dysfunction, arterial stiffening and hypertension associated with ageing (Figure 1). This interesting finding suggests that stem cell-derived EVs may rejuvenate aged arteries. A further study is needed to explore whether EVs extend life-spans of old mice. The use of EVs instead of stem cells as a therapeutic strategy has several advantages. An

obvious advantage is the prospect of a conventional pharmaceutical manufacturing process that is scalable and manageable. The use of EVs also avoids potential complications of stem cell transplants. Our study also provides a potent rationale for further investigation into whether EVs supplements can attenuate age-related arterial stiffening and hypertension in clinical therapy.

We noticed that treatment with EVs decreased systolic BP of old mice to control levels but only partially attenuated arterial stiffening (Figure 1). This observation suggests that the antihypertensive effect of EVs may not be fully mediated by improvement in arterial compliance. By contrast, treatment with EVs nearly abolished ageing-associated impairment in endothelium-dependent vascular relaxation which may, in turn, contribute to its antihypertensive effect. It is interesting that exogenous EVs largely improve vascular endothelial dysfunction associated with ageing.

We further investigated the potential mechanism that mediates the vascular effect of EVs. EVs rescued the downregulation of Sirt1 and eNOS protein expression in vascular intima and media in old mice (Figure 4). Sirt1 is a histone deacetylase that regulates expression of genes related to vascular endothelial cell function [34]. In cultured human aortic endothelial cells (HAECs), we found that EVs upregulated AMPK α and eNOS protein expression and activity (Figure 5), indicating that EVs have direct effect in endothelial cells. AMP-activated protein kinase (AMPK) is a serine/threonine protein kinase that regulates endothelial cell function. Pharmacological activation of AMPK α , a catalytic subunit of AMPK, enhances Sirt1 and eNOS activity and improves klotho deficiency-induced arterial stiffening and hypertension [34]. Thus, the beneficial effects of EVs may be mediated by activation of the Sirt1-AMPK α -eNOS pathway.

Impaired arterial function in the ageing process is implicated by remodelling of arterial structure. Arterial stiffness is one of the earliest adverse structural and functional changes within the vessel wall. The artery wall becomes stiffer over age because of fragmentation and degradation of elastin and subsequent collagen deposition [5,6], resulting in an increase in PWV, an important and reliable measure of arterial stiffness. We further demonstrated that EVs treatment abrogates elastin degradation and collagen deposition in the aortic wall of old mice, accounting for improved vascular function [34]. Mechanistically, ageing increased aortic MMP2 and MMP9 levels (Fig. S6). Upregulation of MMPs, matrix metalloproteinases, destroys the normal matrix structure and promotes vascular remodelling or

fibrosis [35,36]. EVs decreased MMP levels which may contribute to improvement in ageing-associated arterial remodelling. Excessive TGF- β 1, a tissue growth factor, promotes collagen synthesis which may be involved in vascular collagen accumulation [36]. EV treatment decreased TGF- β 1 levels (Fig. S5) which may contribute to its anti-fibrosis effect in old mice. Ageing-associated upregulation of elastase activity may be involved in aortic elastin fragmentation in old mice. EVs inhibited elastase activity which may contribute to its beneficial effect on ageing-associated elastin fragmentation. Smooth muscle cells are the major sources of MMPs, TGF- β 1 and elastase which play important roles in the pathogenesis of vascular stiffness and remodelling [56–58]. These enzymes were synthesized in SMCs and released to the extracellular spaces which regulates matrix structure. Therefore, SMCs may participate in the collagen reduction and elastin preservation in old mice.

We found that EVs also attenuated ageing-related glomerulosclerosis, mesangial matrix expansion, increased collagen deposition, and glomerular collapse. Interestingly, MMP2 and MMP9 levels were upregulated in ageing kidneys (Fig. S9). It has been reported that MMP2 and MMP9 play important roles in the pathogenesis of renal fibrosis and remodelling [59–61]. Thus, the beneficial effect of EVs on renal fibrosis may be partially attributed to the inhibition of MMP2 and MMP9. These improvements in renal degeneration associated with EVs occurred synergistically with the ameliorating vascular function connected to BP regulation. It has been reported that arterial stiffening leads to kidney damage [7,9–11]. This study demonstrated that EVs improved kidney damage. The limitation of this study is that it cannot distinguish whether the beneficial effects of EVs on kidney structural remodelling is the directly associated with EVs treatment or secondary to improvement in arterial stiffness and hypertension. We were unable to quantify plasma EV levels due to the lack of reliable methods. Although EVs at the dose of 18×10^6 effectively attenuated arterial stiffening and hypertension in ageing mice, an additional work is needed to assess the dose-dependent effect of EVs.

Perspective

This study demonstrated that stem cell-derived EVs improved ageing-associated vascular endothelial dysfunction, arterial stiffening, and hypertension, likely via regulating the SIRT1-AMPK α -eNOS pathway. This promising finding warrants clinical validation in aged human subjects. It would be interesting to

investigate whether IV administration of EVs may be an effective therapeutic strategy for vascular diseases associated with ageing. Further studies are required to investigate the components of EVs.

Acknowledgments

We would like to thank Dr. Nathan Tipton for his assistance in editing the manuscript.

Author contributions

Rei Feng, perform experiments and statistical analysis, write manuscript

Mujib Ullah, generate, purify and quantify EVs

Kai Chen, measure vascular activity

Quaisar Ali, measure blood pressure via vascular cannulation

Yi Lin, provide technical support and revise manuscript

Zhongjie Sun, provide conceptual and experimental design, write manuscript, and handling grant funding

Disclosure statement

No potential conflict of interest was reported by the author(s).

Funding

This work was supported by research grants R01 AG049780, AG062375, HL116863, HL 122166, and HL154147 from the National Institutes of Health.

References

- [1] Menotti A, Puddu PE, Tolonen H, et al. Age at death of major cardiovascular diseases in 13 cohorts. The seven countries study of cardiovascular diseases 45-year follow-up. *Acta Cardiol.* 2018;74:1–7.
- [2] Katsuumi G, Shimizu I, Yoshida Y, et al. Vascular senescence in cardiovascular and metabolic diseases. *Front Cardiovasc Med.* 2018;5:18.
- [3] James PA, Oparil S, Carter BL, et al. 2014 evidence-based guideline for the management of high blood pressure in adults: report from the panel members appointed to the Eighth Joint National Committee (JNC 8). *JAMA.* 2014;311:507–520.
- [4] Townsend RR, Wilkinson IB, Schiffrin EL, et al.; American Heart Association Council on H. Recommendations for improving and standardizing vascular research on arterial stiffness: a scientific statement from the American heart association. *Hypertension.* 2015;66:698–722.
- [5] Cavalcante JL, Lima JA, Redheuil A, et al. Aortic stiffness: current understanding and future directions. *J Am Coll Cardiol.* 2011;57:1511–1522.
- [6] Wagenseil JE, Mecham RP. Elastin in large artery stiffness and hypertension. *J Cardiovasc Transl Res.* 2012;5:264–273.

- [7] Sun Z. Aging, arterial stiffness, and hypertension. *Hypertension*. 2015;65:252–256.
- [8] Oh YS, Berkowitz DE, Cohen RA, et al. A special report on the NHLBI initiative to study cellular and molecular mechanisms of arterial stiffness and its association with hypertension. *Circ Res*. 2017;121:1216–1218.
- [9] Sedaghat S, Mattace-Raso FU, Hoorn EJ, et al. Arterial stiffness and decline in kidney function. *Clin J Am Soc Nephrol*. 2015;10:2190–2197.
- [10] Ford ML, Tomlinson LA, Chapman TP, et al. Aortic stiffness is independently associated with rate of renal function decline in chronic kidney disease stages 3 and 4. *Hypertension*. 2010;55:1110–1115.
- [11] Taal MW. Arterial stiffness in chronic kidney disease: an update. *Curr Opin Nephrol Hypertens*. 2014;23:169–173.
- [12] Georgianos PI, Sarafidis PA, Lasaridis AN. Arterial stiffness: a novel cardiovascular risk factor in kidney disease patients. *Curr Vasc Pharmacol*. 2015;13:229–238.
- [13] Liao J, Farmer J. Arterial stiffness as a risk factor for coronary artery disease. *Curr Atheroscler Rep*. 2014;16:387.
- [14] Scuteri A, Brancati AM, Gianni W, et al. Arterial stiffness is an independent risk factor for cognitive impairment in the elderly: a pilot study. *J Hypertens*. 2005;23:1211–1216.
- [15] Jansen F, Nickenig G, Werner N. Extracellular vesicles in cardiovascular disease: potential applications in diagnosis, prognosis, and epidemiology. *Circ Res*. 2017;120:1649–1657.
- [16] Todorova D, Simoncini S, Lacroix R, et al. Extracellular Vesicles in Angiogenesis. *Circ Res*. 2017;120:1658–1673.
- [17] Aikawa E. Extracellular vesicles in cardiovascular disease: focus on vascular calcification. *J Physiol*. 2016;594:2877–2880.
- [18] Osteikoetxea X, Nemeth A, Sodar BW, et al. Extracellular vesicles in cardiovascular disease: are they Jedi or Sith? *J Physiol*. 2016;594:2881–2894.
- [19] Feng B, Ng JH, Heng JC, et al. Molecules that promote or enhance reprogramming of somatic cells to induced pluripotent stem cells. *Cell Stem Cell*. 2009;4:301–312.
- [20] Nordin F, Ahmad RNR, Farzaneh F. Transactivator protein: an alternative for delivery of recombinant proteins for safer reprogramming of induced Pluripotent Stem Cell. *Virus Res*. 2017;235:106–114.
- [21] Rautou PE, Vion AC, Amabile N, et al. Microparticles, vascular function, and atherothrombosis. *Circ Res*. 2011;109:593–606.
- [22] Tetta C, Ghigo E, Silengo L, et al. Extracellular vesicles as an emerging mechanism of cell-to-cell communication. *Endocrine*. 2013;44:11–19.
- [23] Harding CV, Heuser JE, Stahl PD. Exosomes: looking back three decades and into the future. *J Cell Biol*. 2013;200:367–371.
- [24] Kaess BM, Rong J, Larson MG, et al. Aortic stiffness, blood pressure progression, and incident hypertension. *JAMA*. 2012;308:875–881.
- [25] Eirin A, Zhu XY, Puranik AS, et al. Mesenchymal stem cell-derived extracellular vesicles attenuate kidney inflammation. *Kidney Int*. 2017;92:114–124.
- [26] El Harane N, Kervadec A, Bellamy V, et al. Acellular therapeutic approach for heart failure: in vitro production of extracellular vesicles from human cardiovascular progenitors. *Eur Heart J*. 2018;39:1835–1847.
- [27] Liu L, Jin X, Hu CF, et al. Exosomes derived from mesenchymal stem cells rescue myocardial ischaemia/reperfusion injury by inducing cardiomyocyte autophagy via AMPK and Akt pathways. *Cell Physiol Biochem*. 2017;43:52–68.
- [28] Bian S, Zhang L, Duan L, et al. Extracellular vesicles derived from human bone marrow mesenchymal stem cells promote angiogenesis in a rat myocardial infarction model. *J Mol Med (Berl)*. 2014;92:387–397.
- [29] Varshney R, Ali Q, Wu C, et al. Monocrotaline-induced pulmonary hypertension involves downregulation of antiaging protein klotho and eNOS activity. *Hypertension*. 2016;68:1255–1263.
- [30] Lin Y, Chen J, Sun Z. Antiaging gene klotho deficiency promoted high-fat diet-induced arterial stiffening via inactivation of AMP-activated protein kinase. *Hypertension*. 2016;67:564–573.
- [31] Chen K, Zhou X, Sun Z. Haploinsufficiency of klotho gene causes arterial stiffening via upregulation of scleraxis expression and induction of autophagy. *Hypertension*. 2015;66:1006–1013.
- [32] Zhou X, Chen K, Lei H, et al. Klotho gene deficiency causes salt-sensitive hypertension via monocyte chemoattractant protein-1/CC chemokine receptor 2-mediated inflammation. *J Am Soc Nephrol*. 2015;26:121–132.
- [33] Feng M, Whitesall S, Zhang Y, et al. Validation of volume-pressure recording tail-cuff blood pressure measurements. *Am J Hypertens*. 2008;21:1288–1291.
- [34] Gao D, Zuo Z, Tian J, et al. Activation of SIRT1 attenuates klotho deficiency-induced arterial stiffness and hypertension by enhancing AMP-activated protein kinase activity. *Hypertension*. 2016;68:1191–1199.
- [35] Chen K, Sun Z. Activation of DNA demethylases attenuates aging-associated arterial stiffening and hypertension. *Aging Cell*. 2018;e12762. DOI:10.1111/ace1.12762
- [36] Chen K, Sun Z. Autophagy plays a critical role in Klotho gene deficiency-induced arterial stiffening and hypertension. *J Mol Med (Berl)*. 2019;97:1615–1625.
- [37] Wang Q, Zhang M, Ding Y, et al. Activation of NAD(P)H oxidase by tryptophan-derived 3-hydroxykynurenine accelerates endothelial apoptosis and dysfunction in vivo. *Circ Res*. 2014;114:480–492.
- [38] Walker AE, Henson GD, Reihl KD, et al. Greater impairments in cerebral artery compared with skeletal muscle feed artery endothelial function in a mouse model of increased large artery stiffness. *J Physiol*. 2015;593:1931–1943.
- [39] Chen K, Kobayashi S, Xu X, et al. AMP activated protein kinase is indispensable for myocardial adaptation to caloric restriction in mice. *PLoS One*. 2013;8:e59682.
- [40] Lin Y, Sun Z. In vivo pancreatic beta-cell-specific expression of antiaging gene Klotho: a novel approach for preserving beta-cells in type 2 diabetes. *Diabetes*. 2015;64:1444–1458.
- [41] Ullah M, Sun Z. Klotho deficiency accelerates stem cells aging by impairing telomerase activity. *J Gerontol A Biol Sci Med Sci*. 2019;74:1396–1407.
- [42] Chen J, Fan J, Wang S, et al. Secreted klotho attenuates inflammation-associated aortic valve fibrosis in

- senescence-accelerated mice P1. *Hypertension*. 2018;71:877–885.
- [43] Chen J, Lin Y, Sun Z. Deficiency in the anti-aging gene *Klotho* promotes aortic valve fibrosis through AMPK α -mediated activation of *RUNX2*. *Aging Cell*. 2016;15:853–860.
- [44] Wang Y, Sun Z. *Klotho* gene delivery prevents the progression of spontaneous hypertension and renal damage. *Hypertension*. 2009;54:810–817.
- [45] Wang X, Skelley L, Cade R, et al. AAV delivery of mineralocorticoid receptor shRNA prevents progression of cold-induced hypertension and attenuates renal damage. *Gene Ther*. 2006;13:1097–1103.
- [46] Wang X, Skelley L, Wang B, et al. AAV-based RNAi silencing of NADPH oxidase gp91(phox) attenuates cold-induced cardiovascular dysfunction. *Hum Gene Ther*. 2012;23:1016–1026.
- [47] AlGhatrif M, Strait JB, Morrell CH, et al. Longitudinal trajectories of arterial stiffness and the role of blood pressure: the baltimore longitudinal study of aging. *Hypertension*. 2013;62:934–941.
- [48] Laurent S, Cockcroft J, Van Bortel L, et al.; European Network for Non-invasive Investigation of Large A. Expert consensus document on arterial stiffness: methodological issues and clinical applications. *Eur Heart J*. 2006;27:2588–2605.
- [49] Najjar SS, Scuteri A, Shetty V, et al. Pulse wave velocity is an independent predictor of the longitudinal increase in systolic blood pressure and of incident hypertension in the baltimore longitudinal study of aging. *J Am Coll Cardiol*. 2008;51:1377–1383.
- [50] Tsamis A, Krawiec JT, Vorp DA. Elastin and collagen fibre microstructure of the human aorta in ageing and disease: a review. *J R Soc Interface*. 2013;10:20121004.
- [51] Kohn JC, Lampi MC, Reinhart-King CA. Age-related vascular stiffening: causes and consequences. *Front Genet*. 2015;6:112.
- [52] Chen HZ, Wang F, Gao P, et al. Age-associated sirtuin 1 reduction in vascular smooth muscle links vascular senescence and inflammation to abdominal aortic aneurysm. *Circ Res*. 2016;119:1076–1088.
- [53] Ullah M, Sun Z. Stem cells and anti-aging genes: double-edged sword-do the same job of life extension. *Stem Cell Res Ther*. 2018;9:3.
- [54] Wen D, Peng Y, Liu D, et al. Mesenchymal stem cell and derived exosome as small RNA carrier and immunomodulator to improve islet transplantation. *J Control Release*. 2016;238:166–175.
- [55] Hao ZC, Lu J, Wang SZ, et al. Stem cell-derived exosomes: A promising strategy for fracture healing. *Cell Prolif*. 2017;50:e12359.
- [56] Gao F, Chambon P, Offermanns S, et al. Disruption of TGF- β signaling in smooth muscle cell prevents elastase-induced abdominal aortic aneurysm. *Biochem Biophys Res Commun*. 2014;454:137–143.
- [57] Lacolley P, Regnault V, Avolio AP. Smooth muscle cell and arterial aging: basic and clinical aspects. *Cardiovasc Res*. 2018;114:513–528.
- [58] Lacolley P, Regnault V, Segers P, et al. Vascular smooth muscle cells and arterial stiffening: relevance in development, aging, and disease. *Physiol Rev*. 2017;97:1555–1617.
- [59] Racca MA, Novoa PA, Rodriguez I, et al. Renal dysfunction and intragraft proMMP9 activity in renal transplant recipients with interstitial fibrosis and tubular atrophy. *Transpl Int*. 2015;28:71–78.
- [60] Li XM, Peng JH, Sun ZL, et al. Chinese medicine CGA formula ameliorates DMN-induced liver fibrosis in rats via inhibiting MMP2/9, TIMP1/2 and the TGF- β /Smad signaling pathways. *Acta Pharmacol Sin*. 2016;37:783–793.
- [61] Cheng Z, Limbu MH, Wang Z, et al. MMP-2 and 9 in Chronic Kidney Disease. *Int J Mol Sci*. 2017;18:776–780.

Novelty and Significance

What is new?

- This study reported for the first time that stem cell-derived extracellular vesicles (EVs) attenuate ageing-associated endothelial dysfunction, arterial stiffness and hypertension.
- This study establishes an interesting link between EVs and the SIRT1-AMPK α -eNOS pathway.

(1) What is relevant?

- There is currently no effective intervention for ageing-associated cardiovascular disorders such as endothelial dysfunction, arterial stiffness and hypertension.
- This study reveals that IV delivery of EVs may be an effective therapy for ageing-associated endothelial dysfunction, arterial stiffness and hypertension.

(1) Summary

This study provides the first evidence that stem cell-derived EVs attenuate ageing-associated endothelial dysfunction, arterial stiffness and hypertension. The beneficial effect of EVs maybe mediated by upregulation of the Sirt1-AMPK α -eNOS pathway. This promising finding warrants clinical validation in aged human subjects.